γ-ray spectroscopy of ^{132}Te through β decay of a ^{132}Sb radioactive beam

R. O. Hughes,[1,2] N. V. Zamfir,[1,3,4] D. C. Radford,[5] C. J. Gross,[5] C. J. Barton,[6] C. Baktash,[5] M. A. Caprio,[1,7] R. F. Casten,[1] A. Galindo-Uribarri,[5] P. A. Hausladen,[5] E. A. McCutchan,[1] J. J. Ressler,[1] D. Shapira,[5] D. W. Stracener,[5] and C.-H. Yu[5]

[1]*Wright Nuclear Structure Laboratory, Yale University, New Haven, Connecticut 06520-8124, USA*
[2]*Department of Physics, University of Surrey, Guildford GU2 7XH, United Kingdom*
[3]*Clark University, Worcester, Massachusetts 01610, USA*
[4]*Institutul Naţional de Fizică şi Inginerie Nucleară, RO-76900 Bucureşti-Măgurele, Romania*
[5]*Physics Division, Oak Ridge National Laboratory, Oak Ridge, Tennessee 37831, USA*
[6]*University of York, Heslington, YO10 5DD, United Kingdom*
[7]*Center for Theoretical Physics, Sloane Physics Laboratory, Yale University, New Haven, Connecticut 06520-8120, USA*

(Received 28 December 2004; published 26 April 2005)

γ-ray spectroscopy of ^{132}Te, obtained from β^- decay of a ^{132}Sb radioactive beam at the Holifield Radioactive Ion Beam Facility, was performed using the Clarion array. A significantly revised γ-decay scheme for ^{132}Te was obtained including a number of new, likely 2^+, states below 2.5 MeV and the removal of a 3^- state at 2280 keV. A simple shell-model interpretation is discussed for the low-lying levels.

DOI: 10.1103/PhysRevC.71.044311 PACS number(s): 21.10.−k, 21.60.Cs, 23.20.Lv, 27.60.+j

I. INTRODUCTION

The availability of high-intensity β-decay activities at the Holifield Radioactive Ion Beam Facility (HRIBF) at Oak Ridge provides a means of improving the quality of γ-ray spectroscopy data on neutron-rich nuclei. One of the most interesting and, at the same time, most accessible regions is that near the doubly magic ^{132}Sn. Coulomb excitation experiments in this region [1–3] making use of radioactive beam scattering in inverse kinematics have allowed a systematic study of the quadrupole collectivity and discovered an unusual behavior: in ^{136}Te both the 2_1^+ energy and the $B(E2; 0_1^+ \to 2_1^+)$ transition strength are lower than in ^{132}Te. This contradicts the general intuition that a decreasing 2_1^+ energy should be accompanied by an increasing $B(E2; 0_1^+ \to 2_1^+)$ value. The experimental anomaly was explained by Terasaki *et al.* [4] by using a pairing strength dependent on single-particle level density.

This paper presents new decay data on ^{132}Te populated in β^- decay and studied through γ-ray coincidence spectroscopy. The details of the experiment and the results are presented in Sec. II. The low-lying levels in the ^{132}Te nucleus can be, at least qualitatively, explained in terms of the shell model as coupling two protons and two neutron holes to the doubly closed shell nucleus ^{132}Sn. A short discussion on the structure of some selected levels is presented in Sec. III. Some of this material has been summarized previously [5].

II. EXPERIMENT AND RESULTS

Low-lying levels of ^{132}Te were populated in the β^- decay of ^{132}Sb. A radioactive ^{132}Sb beam at 396 MeV and with an intensity of $\sim 10^7$ particles/s was provided by the HRIBF, from proton-induced fission of uranium. The beam was embedded in a thick foil target (14.3 mg/cm^2 Al + 1.0 mg/cm^2 C) and the γ rays following β decay were observed with the Clarion array [6]. Decay experiments such as this can be carried out using the experimental setup from Coulomb excitation experiments [1,2] with minimal modification, that is, essentially the substitution of a stopper foil for the excitation foil, and can thus productively be performed in conjunction with such experiments. The beam energy used is not an essential requirement, but is chosen simply to be sufficiently below the Coulomb barrier to avoid production of background radiation.

The Clarion array [6] consists of 11 clover Ge detectors equipped with BGO Compton suppression shields. The array surrounds a 15-cm radius target chamber. Most of the detectors were located in the back hemisphere of the array, approximately 25 cm from the target, with a 2.3% total array photopeak efficiency at 1.33 MeV. The experiment was run for 16 h with a $\gamma - \gamma$ doubles or higher fold trigger. Singles γ-ray data were also briefly acquired. A total of $\sim 4.0 \times 10^6$ singles events and $\sim 2.5 \times 10^7$ coincidence events were collected.

The singles spectrum obtained in the present work is shown in Fig. 1. The observed γ rays in ^{132}Te, their relative intensity, and the most useful coincidence relations in building the decay scheme are listed in Table I. The intensities were calculated from singles and coincidence data following procedures similar to those in Ref. [7]. Due to the high statistics, the lowest measurable transition intensity was reduced by more than an order of magnitude from the previous ~ 0.5 γ rays per 100 decays [8] to ~ 0.02 per 100 decays.

The ^{132}Sb parent nuclei decay via two β^- channels, from the 4^+ ground state ($T_{1/2} = 2.8$ m) and an 8^- excited state ($T_{1/2} = 4.2$ m). Thus, levels of a relatively wide spin range could be populated. Continuous beam deposition was used to provide maximal statistics. Therefore, no attempt was made to separate the γ rays originating from the two different parent states on the basis of decay curves.

Multiple isomeric states are present in ^{132}Te. As a conventional coincidence condition was imposed in the triggering electronics, the experiment provided at most limited sensitivity to coincidences between γ-ray transitions populating and depopulating levels with lifetimes greater than a few microseconds. Thus, coincidences between transitions deexciting the

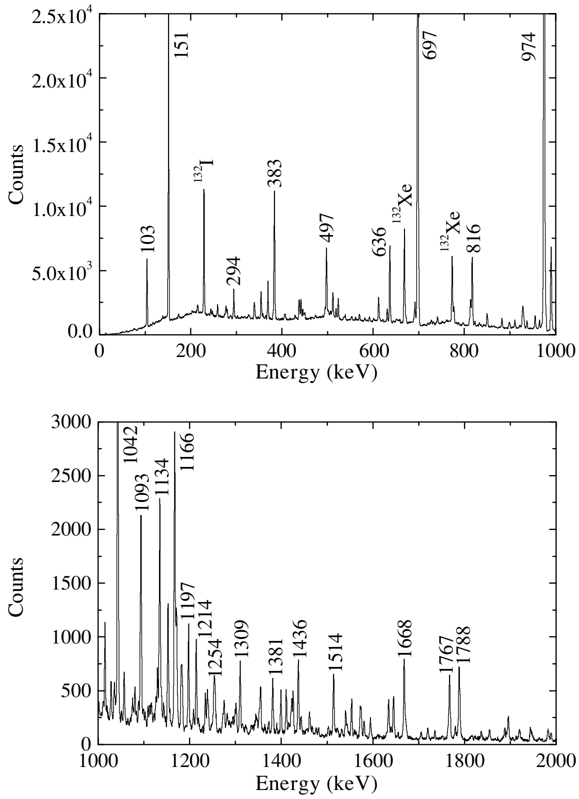

FIG. 1. γ-ray spectrum observed in the present work following the β decay of ^{132}Sb. Some strong transitions from ^{132}Te are marked by their energy in keV. The strongest of the contaminant lines are indicated by their origin.

145-ns isomeric state at 1775 keV [9] and transitions feeding this level could be observed, but no coincidence events were registered between transitions below and above the 1925 keV state ($T_{1/2} = 28\,\mu$s).

The new γ-γ coincidence data have led to a revised γ-decay scheme for ^{132}Te with many new transitions and new levels. A number of previous placements were found to be inconsistent with the new high-quality coincidence data. A complete summary of the levels populated in ^{132}Te and their γ-ray decays are listed in Table II. Partial results were reported in Ref. [5]. Some of the results obtained here have been corroborated in the unpublished work of Ref. [10]. Figure 2 highlights the levels observed below 2500 keV as deduced in this work, including a comparison with the previously reported β-decay level scheme [8]. Changes to the level scheme below 2400 keV are discussed in detail below. Intensities given in the following discussion are normalized to the intensity of the 974 keV, $2_1^+ \rightarrow 0_1^+$, γ-ray transition ($I_{974} \equiv 1000$).

(2_2^+) *at 1665 keV.* We observe a new state at 1665 keV, nearly degenerate with the 4_1^+ state at 1671 keV, decaying by a 690.96(10) keV transition with intensity 20(3) to the 2_1^+ level and by a very weak 1665.3(2) keV transition with intensity 0.2(1) to the ground state. The level is observed to have nine populating transitions (see Table I), three of which are reasonably strong: 822, 936, and 1098 keV. Coincidence spectra gated on the 822 keV feeding transition and on the 691 and 1665 keV depopulating transitions are given in Fig. 3. Based on the transitions to only the 2_1^+ and 0_1^+ states, we tentatively give the level at 1665 keV a 2^+ assignment. Three additional levels (1788, 2249, and 2364 keV), discussed in detail below, also decay only to the 2_1^+ and 0_1^+ levels. A simple interpretation in terms of the shell model (see below) supports a likely 2^+ assignment to each of these levels.

(2_3^+) *at 1788 keV.* The level at 1788 keV was identified on the basis of several transitions. Two depopulating transitions, an 813.25(10) keV line with intensity 23(1) and a 1787.6(3) keV line with intensity 16(1) to the 2_1^+ and 0_1^+ levels, respectively, were observed along with eight populating transitions. A gate on one of the strongest populating transitions, a 2587.1(4) keV line with intensity 3.6(9), is given in Fig. 4, illustrating coincidences with the 813 and 1788 keV depopulating transitions. Support for the spin assignment of this level will be discussed in detail below.

(5_1^-) *at 2054 keV.* The 5_1^- state at 2054 keV was previously reported to decay to the 4_1^+ state through a transition of 383 keV [9]. This transition was observed and confirmed to have an intensity consistent with the literature intensity with some reduction in the uncertainty. Evidence was found for an additional depopulating transition, of 279.09(9) keV with intensity 5.3(2), to the 6_1^+ state. This new transition is consistent with the previous spin assignment of 5_1^-.

Level at 2192 keV. A level 2191.93(22) keV is observed on the basis of one populating and one depopulating transition. The prior β-decay study [8] places a 138.5 keV transition, with intensity 7.0(20), tentatively depopulating a level at 3349 keV. Our coincidence data find a 138.05(8) keV transition with intensity 6.5(9) as depopulating a new level at 2192 keV. This placement is supported by additional coincidence relations (see Table I).

(2_4^+) *at 2249 keV.* A new level at 2249 keV is identified on the basis of two depopulating transitions and two weak populating transitions. The level is observed to decay to the 2_1^+ and 0_1^+ states via a 1274.6(2) keV line with intensity 5.0(5) and a 2248.8(6) keV line with intensity 0.3(2), respectively. A 1274.6 keV line was observed with an intensity of 12(2) in the prior β-decay study, but it was not given a placement within the level scheme of ^{132}Te.

(3_1^-) *at 2281 keV.* A 3_1^- level was previously reported at 2281 keV [8,9]. The placement was based primarily on three transitions, 610 keV with intensity 20(4), 1306 keV with intensity 10(2), and 2280 keV with intensity 10(2), from this level to the 4_1^+, 2_1^+, and 0_1^+ states, respectively. These intensities yield a huge value for the corresponding $B(E3)$ of the $3^- \rightarrow 0_1^+$ transition. From the reported literature values [9], the ratio $B(E1; 3^- \rightarrow 2^+)/B(E3; 3^- \rightarrow 0^+)$ gives 3×10^{-8}. Assuming a $B(E1; 3^- \rightarrow 2^+)$ value of $\sim 10^{-4}$ W.u., which is typical for transitions of this kind in this region [11], the $B(E3; 3^- \rightarrow 0^+)$ would have been $\sim 10^4$ W.u., two orders of magnitude larger than any other known value. If this was indeed the decay mode of this state, it would have presented a challenge to our understanding of negative parity excitations.

TABLE I. Observed γ-ray transitions in ^{132}Te, arranged in order of increasing transition energy. Intensities (normalized to $I_{974} \equiv 1000$) and the most useful coincidence relations are given.

E_γ (keV)	I	E_i (keV)	E_f (keV)	Coincidences (keV)
103.36(8)	611(131)	1774.69	1671.34	151,354,636,697,974,990,1152,1197,1436
124.2(2)[a]	1.2(4)	3091.7	2967.4	383,1042
138.05(8)[b]	6.5(9)	2191.93	2053.88	383,697,974
143.0(3)[a]	0.7(3)	3234.8	3091.7	1042,1166
150.54(7)	436(61)	1925.23	1774.69	103,697,974
172.2(2)[a]	2.6(6)	3478.1	3305.9	338,964,1042,1129
214.22(9)[a]	6(1)	3305.9	3091.7	287,1136,1166,1207,1301
237.8(4)[a]	0.8(6)	2601.8	2363.7	1389.2363
243.7(2)[a]	2.3(8)	3335.5	3091.7	258,849,921,1014,1166
257.61(8)[a]	3.5(5)	3593.1	3335.5	244,670,849,921,1014,1166,1410
273.7(4)[a]	2.3(7)	3241.1	2967.4	441,449,740,760,1042
276.45(7)[b]	8.4(8)	2764.37	2487.9	380,691,697,817,822,974,1514
279.09(9)[a]	5.3(2)	2053.88	1774.69	103,369,611,697,974,1181
287.1(3)[a]	1.4(10)	3593.1	3305.9	214,338,849,1014,1042,1381
293.62(7)[c]	18(1)	3261.0	2967.4	441,449,733,740,1042,1346,1453
301.4(4)[a]	0.4(2)	2854.5	2553.2	437,445,882,1134
325.6(3)[a]	2.0(6)	3210.4	2884.8	697,777,974,1214
338.55(9)[a]	9(1)	3305.9	2967.4	173,287,441,494,696,689,1042,1137,1207
353.69(8)	19(1)	2764.37	2410.6	103,636,697,974
356.78(9)[a]	2.8(5)	3211.1	2854.5	103,697,731,844,974,1080,1183
363.25(12)[a]	1.4(9)	2971.5	2608.2	500,1134,1634
368.49(9)	24(2)	2422.3	2053.88	243,279,383,697,813,928,974,1056,1171
379.9(1)[a]	3.7(4)	2487.9	2108.05	276,437,697,974,1134,1887
382.65(9)	74(4)	2053.88	1671.34	138,369,385,611,697,974,1181,1281,2022
383.2(2)[a]	9(1)	3350.5	2967.4	911,1042,1092
384.93(9)[a]	2.7(6)	2576.9	2191.93	138,279,383,697,974
399.9(9)[a]	0.8(2)	2763.6	2363.7	974,1389,2363
406.75(10)[a]	1.6(6)	3015.1	2608.2	500,1134,1634
436.72(8)	14(1)	2108.05	1671.34	380,445,500,656,697,777,907,974
440.98(8)[a]	14(1)	4442.6	4001.6	273,294,338,518,538,696,740,760,1034
443.7(3)[a]	0.7(2)	2854.5	2410.6	103,636,697,974
445.09(8)[a]	7(1)	2553.2	2108.05	437,697,974,1076,1134,1338,1502,1574
449.3(1)[a]	4.2(3)	3710.3	3261.0	273,294,518,538,1042
493.7(4)[a]	0.4(2)	2601.8	2108.05	437,1134
493.95(8)[a]	3.4(5)	4488.7	3994.8	294,338,689,733,1027,1042
496.96(8)	48(3)	2422.3	1925.23	243,813,928,1056,1171,1271,1581,2166
500.1(2)[a]	3.3(5)	2608.2	2108.05	363,437,1134
501.3(2)[a]	2.4(6)	3593.1	3091.7	849,1014,1166
510.96(8)[a]	10.9(14)	3478.1	2967.4	964,1042,1129
523.24(10)[a]	4(1)	2576.9	2053.88	383,279,697,974
552.0(2)[a]	3.0(5)	3519.1	2967.4	1042
560.9(2)[a]	2.5(5)	2971.5	2410.6	103,591,636,658,697,974
568.8(2)[a]	1.6(4)	4262.5	3693.7	1767
569.6(5)[a]	3.4(5)	3234.8	2665.2	383,611,1254,1354
591.09(9)[a]	3.3(7)	3562.5	2971.5	561,636,1197,1300
611.36(9)[b]	19(1)	2665.2	2053.88	279,383,570,670,928
635.9(1)	62(3)	2410.6	1774.69	103,354,561,697,974,1108,1115,1152
655.7(3)[a]	1.9(6)	2763.6	2108.05	437,1134
657.6(3)[a]	1.1(4)	3629.4	2971.5	561,636,1197,1300
667.9(3)[a]	0.7(3)	4260.9	3593.1	258,287,501,928,1171,1668
670.3(3)[a]	0.9(4)	3335.5	2665.2	258,611
688.8(2)[a]	3.1(5)	3994.8	3305.9	338,494
690.96(10)[a]	20(3)	1665.30	974.34	276,822,936,974,1098,2717,2919
695.9(2)[a]	3.1(5)	4001.6	3305.9	338,441
697.0(1)	873(40)	1671.34	974.34	103,151,383,437,817,974,990,1093
700.1(3)[a]	0.6(1)	2487.9	1787.6	813,1787

TABLE I. (*Continued.*)

E_γ (keV)	I	E_i (keV)	E_f (keV)	Coincidences (keV)
723.5(4)[a]	2.3(5)	3211.1	2487.9	817,974,1514
730.9(3)[a]	2.4(6)	3942.1	3211.1	357,1437,1540
733.0(3)[a]	1.0(3)	3994.8	3261.0	294,494,1042
737.3(2)[a]	1.2(8)	3254.8	2517.4	974,1543
740.5(1)[a]	6.0(6)	4001.6	3261.0	273,294,441,518,538,1042
750.6(2)[a]	1.4(4)	4443.5	3693.7	1767
760.4(2)[a]	2.0(8)	4001.6	3241.1	273,441,518
776.7(2)[b]	5(1)	2884.8	2108.05	326,437,1134
782.5(4)[a]	0.4(2)	4260.9	3478.1	511,1042,1553
796.6(2)[a]	1.8(4)	4490.3	3693.7	1767
798.2(5)[a]	0.3(2)	3562.5	2764.37	990,103,697,974
812.54(10)[a]	4.8(6)	3234.8	2422.3	369,497,1254,1354
813.25(10)[b]	23(1)	1787.6	974.34	974,2587
814.2(3)[a]	0.6(3)	2601.8	1787.6	813,1787
816.56(10)	68(4)	2487.9	1671.34	276,697,724,974,1887
821(1)[a]	<0.2	2608.2	1787.6	813,1787
822.6(1)[a]	3.4(3)	2487.9	1665.30	691,974
841.1(4)[a]	0.9(3)	4534.8	3693.7	1767
844.1(2)[a]	1.6(4)	4055.4	3211.1	357,1437,1540
849.5(1)[a]	12(1)	4442.6	3593.1	258,287,501,928,1171,1668
881.8(1)[b]	9(1)	2553.2	1671.34	697,974,1076,1338,1502,1574
907.0(4)[a]	1.4(4)	3015.1	2108.05	437,1134
910.2(2)[a]	1.2(4)	4260.9	3350.5	383,929,1426
921.1(2)[a]	2.8(7)	4513.8	3593.1	258,287,501,928,1171,1668
927.9(4)[a]	3.2(6)	3593.1	2665.2	611,849,921,1014
930.3(3)[a]	6.6(11)	2601.8	1671.34	697,974
936.5(2)[a]	4.3(5)	2601.8	1665.30	691,974
936.9(2)[a]	4(1)	2608.2	1671.34	697,974
955(1)[a]	0.5(3)	4260.9	3305.9	338,1381
964.2(2)[a]	7(1)	4442.6	3478.1	173,511,1056,1553
974.34(10)	1000(50)	974.34	0.0	691,697,813,1134,1275,1389,1513
989.67(11)	91(6)	2764.37	1774.69	103,697,974
1014.25(11)[a]	10(1)	4607.3	3593.1	258,287,501,928,1171,1668
1027.4(2)[a]	4.3(7)	3994.8	2967.4	494,1042
1034.2(2)[a]	3.9(6)	4001.6	2967.4	441,1042
1042.1(1)[b]	74(4)	2967.4	1925.23	294,273,338,1027,1034
1055.96(11)[a]	4.8(9)	3478.1	2422.3	369,497,964,1129
1056.7(3)[a]	1.4(4)	3821.1	2764.37	354,990
1076.2(2)[a]	1.7(10)	3629.4	2553.2	437,445,882,1134
1079.77(12)[a]	2.6(4)	2854.5	1774.69	103,357,1088,1201
1087.76(13)[a]	2.7(6)	3942.1	2854.5	103,697,974,1080,1183
1092.0(3)[a]	1.8(6)	4442.6	3350.5	383,929,1426
1093.04(11)[b]	28(2)	2764.37	1671.34	697,974
1098.3(2)[a]	1.7(4)	2763.6	1665.30	691,974
1103.2(4)[a]	0.5(2)	3211.1	2108.05	437,1134
1108.5(2)[a]	2.5(6)	3519.1	2410.6	103,636,697,974
1114.5(3)[a]	1.3(9)	3525.1	2410.6	103,636,697,974
1120.7(4)[a]	0.5(2)	3722.3	2601.8	813,930,936
1126.5(3)[a]	0.9(4)	3891.6	2764.37	990
1129.0(2)[a]	6(1)	4607.3	3478.1	173,511,1056,1553
1133.8(2)	34(2)	2108.05	974.34	380,445,500,656,777,974
1136.66(18)[a]	0.9(3)	4442.6	3305.9	214,338,1381
1151.85(16)	21(1)	3562.5	2410.6	103,636,697,974
1166.46(13)	22(1)	3091.7	1925.23	214,243,501,1169,1351
1169.2(3)[a]	8(1)	4260.9	3091.7	1166
1170.9(2)[a]	13.8(30)	3593.1	2422.3	369,497,849,921,1014
1181.0(2)[a]	9(1)	3234.8	2053.88	279,383,1254,1354

TABLE I. (*Continued.*)

E_γ (keV)	I	E_i (keV)	E_f (keV)	Coincidences (keV)
1181.6(3)[a]	1.3(4)	4442.6	3261.0	294,1042
1183.3(3)[c]	6.4(6)	2854.5	1671.34	357,697,974,1088,1201
1196.7(2)[b]	9.5(7)	2971.5	1774.69	103,591,658,697,974
1200.9(13)[a]	0.6(4)	4055.4	2854.5	1080,1183
1207.64(18)[a]	2.6(9)	4513.8	3305.9	214,338,1381
1213.55(12)	14(1)	2884.8	1671.34	326,697,974
1219.0(5)[a]	<0.5	3629.4	2410.6	636
1219.6(6)[a]	0.2(1)	2884.8	1665.30	691,974
1227.7(9)[a]	<0.2	3015.1	1787.6	813,1787
1238.0(6)[a]	0.2(1)	4588.5	3350.5	383,929,1426
1238.01(2)[a]	4.3(5)	3660.3	2422.3	369,497
1240.1(6)[a]	3(1)	3015.1	1774.69	103,697,974
1246.6(4)[a]	0.7(2)	2917.9	1671.34	697,974
1252.6(4)[a]	0.8(2)	2917.9	1665.30	691,974
1254.1(2)[a]	3.3(6)	4488.7	3234.8	570,813,1181,1310
1271.4(3)[a]	2.1(9)	3693.7	2422.3	369,497
1274.6(2)[c]	5.0(5)	2248.9	974.34	974,2126,2166,2218,2284
1281.8(3)[a]	2.2(14)	3335.5	2053.88	279,383
1291.0(8)[a]	0.2(1)	4055.4	2764.37	354,990,1093
1293.3(3)[a]	1.5(5)	4260.9	2967.4	1042
1300.2(2)[a]	4.4(5)	2971.5	1671.34	591,658,697,974
1301.4(3)[a]	1.0(3)	4607.3	3305.9	214,338,1381
1309.46(13)[a]	12(1)	3234.8	1925.23	1254,1354
1321.3(2)[a]	1.1(3)	3429.4	2108.05	437,1134
1338.8(3)[a]	<1	3891.6	2553.2	445,882
1343.6(3)[a]	2.0(5)	3015.1	1671.34	697,974
1346.3(2)[a]	2.4(5)	4607.3	3261.0	273,294,518,538
1351.05(15)[a]	3.2(6)	4442.6	3091.7	1166
1353.95(16)[a]	7(1)	4588.5	3234.8	570,813,1181,1310
1358.6(4)[a]	0.6(4)	3722.3	2363.7	974,1389,2363
1380.7(2)	10(1)	3305.9	1925.23	287,689,696,1136,1207
1380.8(3)[a]	1.6(4)	3488.3	2108.05	437,1134
1389.5(2)[a]	1.2(7)	2363.7	974.34	238,400,974,1359,1524,2011
1409.8(5)[a]	0.5(3)	4173.8	2764.37	990,
1410.2(2)[a]	8(1)	3335.5	1925.23	258,849,921,1014
1422.0(2)[a]	5(1)	4513.8	3091.7	1166
1425.3(2)[a]	5.6(7)	3350.5	1925.23	910,1092
1436.45(14)	13.4(16)	3211.1	1774.69	697,731,844,974
1453.2(3)[a]	0.4(2)	4714.2	3261.0	294
1454.5(3)	0.9(4)	3562.5	2108.05	437,1134
1475.0(3)[a]	1.5(5)	4442.6	2967.4	1042
1480.1(4)[a]	0.6(2)	3891.6	2410.6	103,636,697,974
1502.3(2)[a]	1.5(5)	4055.4	2553.2	437,445,882,1134
1513.6(1)	12.4(12)	2487.9	974.34	276,724,974,1887
1521.2(4)[a]	1.4(4)	3629.4	2108.05	437,697,974,1134
1523.5(3)[a]	1.2(8)	3887.1	2363.7	1389,2363
1531.6(3)[a]	1.3(3)	3942.1	2410.6	103,636,697,974
1539.6(3)	4.8(14)	3211.1	1671.34	697,731,844,974
1543.1(2)[a]	1.4(6)	2517.4	974.34	737,974
1553.1(2)[a]	7(1)	3478.1	1925.23	964,1129
1574.0(2)[b]	4.3(5)	4127.0	2553.2	437,445,882,1134
1579.8(2)[a]	3.0(10)	4002.1	2422.3	369,383,497
1633.9(2)[c]	7(1)	2608.2	974.34	363,974
1644.5(2)[c]	9(1)	4055.4	2410.6	103,636,697,974
1665.3(2)[a]	0.2(1)	1665.30	0.0	822,936,1098
1667.9(2)[a]	17.9(19)	3593.1	1925.23	849,921,1014
1763.2(4)[c]	2.2(6)	4173.8	2410.6	103,636,697,974

TABLE I. (*Continued*.)

E_γ (keV)	I	E_i (keV)	E_f (keV)	Coincidences (keV)
1766.9(3)[a]	14(1)	3693.7	1925.23	569,751,797,841
1787.6(3)[b]	16(1)	1787.6	0.0	2587
1815.7(4)[a]	0.8(3)	4305.3	2487.9	817,1514
1822.1(4)[a]	0.6(3)	4488.7	2665.2	383,611
1854.3(3)[c]	2.5(5)	3629.4	1774.69	103,697,974
1887.2(4)[a]	2.9(9)	4375.1	2487.9	380,817,822,1514
1890(1)[b]	0.6(3)	3942.1	2053.88	383
1894.6(4)[b]	0.9(3)	4305.3	2410.6	103,636,697,974
1924.8(8)[a]	<0.4	4533.0	2608.2	500,1134,1634
1943.5(4)[a]	3.3(7)	2917.9	974.34	974
1947.2(3)[a]	1.8(5)	4055.4	2108.05	437,697,974,1134
1988.9(4)[a]	1.6(6)	4654.1	2665.2	383,611
2011.3(8)[a]	<0.4	4375.1	2363.7	1389,2363
2018.8(5)[a]	2.4(6)	4127.0	2108.05	437,697,974,1134
2022.9(6)[a]	1.2(11)	4076.8	2053.88	383,697,974
2032.7(5)[a]	1.1(5)	4443.5	2410.6	103,636,697,974
2040.8(6)[a]	0.9(3)	3015.1	974.34	974
2071(1)[a]	<0.2	3858.1	1787.6	813,1787
2100(1)[a]	<0.2	3887.1	1787.6	813,1787
2116.1(4)[a]	1.5(4)	3891.6	1774.69	103,697,974
2126(2)[a]	0.7(4)	4375.1	2248.9	974,1275
2166.0(8)[a]	1.3(5)	4588.5	2422.3	369,383,497,697,974
2166(2)[a]	0.6(4)	4415.3	2248.9	974,1275
2181.5(9)[a]	<0.4	4604.6	2422.3	369,383,497
2187(1)[a]	0.6(3)	3858.1	1671.34	697,974
2194.0(8)[a]	1.2(5)	4604.6	2410.6	103,636,697,974
2197.2(5)[a]	1.3(10)	4305.3	2108.05	437,697,974,1134
2219(2)[a]	<0.4	4467.7	2248.9	974,1275
2221.5(9)[a]	<0.5	4585.2	2363.7	974,1389,2363
2222(1)[a]	0.5(2)	3887.1	1665.30	691,974
2225(1)[a]	0.4(2)	4890	2665.2	383,611
2248.8(6)[a]	0.3(2)	2248.9	0.0	2126,2166,2218
2280.2(5)[b]	2.1(5)	4054.9	1774.69	103,697,974
2284.2(5)[a]	<0.4	4533.0	2248.9	974,1275
2307.4(7)[a]	1.1(4)	4415.3	2108.05	437,697,974,1134
2360.7(5)[a]	0.5(3)	4468.8	2108.05	437,697,974,1134
2363.5(3)[a]	3.6(4)	2363.7	0.0	238,400,1359,1524,2011,2221
2383.6(3)[a]	3.3(14)	4054.9	1671.34	697,974
2413.7(7)[a]	<0.5	4467.7	2053.88	383,697,974
2455(1)[a]	<0.5	4127.0	1671.34	697,974
2477.0(3)[a]	2.3(9)	4585.2	2108.05	437,697,974,1134
2513.9(6)[a]	1.7(9)	3488.3	974.34	974
2563.0(3)[a]	3.8(10)	4337.7	1774.69	103,697,974
2587.1(4)[b]	3.6(9)	4375.1	1787.6	813,974,1788
2633.0(4)[c]	2.6(5)	4685.9	2053.88	279,383,697,974
2665.0(6)[c]	1.9(4)	4439.6	1774.69	103,697,974
2695.0(8)[a]	0.6(2)	4748.9	2053.88	383,697,974
2703.4(7)[a]	1.2(4)	4375.1	1671.34	697,974
2710.9(7)[a]	2.3(7)	4382.2	1671.34	697,974
2717.0(9)[a]	<0.5	4382.2	1665.30	691,974
2762.7(8)[a]	0.4(2)	4433.5	1671.34	697,974
2797(1)[a]	<0.3	4584	1787.6	813,1787
2801(1)[a]	<0.3	4467.7	1665.30	691,974
2829.2(7)[a]	1.7(5)	4604.6	1774.69	103,697,974
2912.0(5)[c]	3.5(5)	3887.1	974.34	974
2919.0(8)[a]	1.6(5)	4584	1665.30	691,974
3329(2)[a]	<0.5	4305.3	974.34	974

TABLE I. (*Continued.*)

E_γ (keV)	I	E_i (keV)	E_f (keV)	Coincidences (keV)
3351(1)[a]	0.8(5)	4325.2	974.34	974
3407(2)[a]	0.5(2)	4382.2	974.34	974
3459(1)[a]	1.3(7)	4433.5	974.34	974
3558.0(5)[a]	2.7(6)	4533.0	974.34	974
3610(2)[a]	0.7(4)	4584	974.34	974
3700(2)[a]	0.3(2)	4674	974.34	974

[a]γ-ray line was not previously reported.
[b]γ-ray line was not reported in this placement.
[c]Previously unplaced.

TABLE II. Level populated in ^{132}Te and their γ-ray decay. Intensities (normalized to $I_{974} \equiv 1000$) are given for γ-ray transitions depopulating the levels. Assigned spin values are also given.

E_i (keV)	J_i^π	E_γ (keV)	I	E_f (keV)	J_f^π
974.34(10)	2^+	974.34(10)	1000(50)	0.0	0^+
1665.30(14)[a]	(2^+)	690.96(10)	20(3)	974.34	2^+
		1665.3(2)	0.2(1)	0.0	0^+
1671.34(14)	4^+	697.0(1)	873(40)	974.34	2^+
1774.69(16)	6^+	103.36(8)	611(131)	1671.34	4^+
1787.6(2)[a]	(2^+)	813.25(10)	23(1)	974.34	2^+
		1787.6(3)	16(1)	0.0	0^+
1925.23(17)	$(7)^-$	150.54(7)	436(61)	1774.69	6^+
2053.88(16)	$(5)^-$	279.09(9)	5.3(2)	1774.69	6^+
		382.65(9)	74(4)	1671.34	4^+
2108.05(18)	(3,4)	436.72(8)	14(1)	1671.34	4^+
		1133.8(2)	34(2)	974.34	2^+
2191.93(22)[a]		138.05(8)	6.5(9)	2053.88	$(5)^-$
2248.9(2)[a]	(2^+)	1274.6(2)	5.0(5)	974.34	2^+
		2248.8(6)	0.3(2)	0.0	0^+
2363.7(2)[a]	(2^+)	1389.5(2)	1.2(7)	974.34	2^+
		2363.5(3)	3.6(4)	0.0	0^+
2410.6(2)		635.9(1)	62(3)	1774.69	6^+
2422.3(2)		368.49(9)	24(2)	2053.88	$(5)^-$
		496.96(8)	48(3)	1925.23	$(7)^-$
2487.9(2)	(3,4)	379.9(1)	3.7(4)	2108.05	(3,4)
		700.1(3)	0.6(1)	1787.6[a]	(2^+)
		816.56(10)	68(4)	1671.34	4^+
		822.6(1)	3.4(3)	1665.30[a]	(2^+)
		1513.6(1)	12.4(12)	974.34	2^+
2517.4(2)[a]		1543.1(2)	1.4(6)	974.34	2^+
2553.2(2)[a]		445.09(8)	7(1)	2108.05	(3,4)
		881.8(1)	9(1)	1671.34	4^+
2576.9(3)[a]		384.93(9)	2.7(6)	2191.93[a]	
		523.24(10)	4(1)	2053.88	$(5)^-$
2601.8(3)[a]		237.8(4)	0.8(6)	2363.7[a]	(2^+)
		493.7(4)	0.4(2)	2108.05	(3,4)
		814.2(3)	0.6(3)	1787.6[a]	(2^+)
		930.3(3)	6.6(11)	1671.34	4^+
		936.5(2)	4.3(5)	1665.30[a]	(2^+)

TABLE II. (*Continued*.)

E_i (keV)	J_i^π	E_γ (keV)	I	E_f (keV)	J_f^π
2608.2(2)[a]		500.1(2)	3.3(5)	2108.05	(3,4)
		821(1)	<0.2	1787.6[a]	(2^+)
		936.9(2)	4(1)	1671.34	4^+
		1633.9(2)	7(1)	974.34	2^+
2665.2(3)[a]		611.36(9)	19(1)	2053.88	$(5)^-$
2763.6(3)[a]	$(3,4^+)$	399.9(9)	0.8(2)	2363.7[a]	(2^+)
		655.7(3)	1.9(6)	2108.05	(3,4)
		1098.3(2)	1.7(4)	1665.30[a]	(2^+)
2764.37(15)	(4,5)	276.45(7)	8.4(8)	2487.9	(3,4)
		353.69(8)	19(1)	2410.6	
		989.67(11)	91(6)	1774.69	6^+
		1093.04(11)	28(2)	1671.34	4^+
2854.5(3)[a]		301.4(4)	0.4(2)	2553.2[a]	
		443.7(3)	0.7(2)	2410.6	
		1079.77(12)	2.6(4)	1774.69	6^+
		1183.3(3)	6.4(6)	1671.34	4^+
2884.8(3)		776.7(2)	5(1)	2108.05	(3,4)
		1213.55(12)	14(1)	1671.34	4^+
		1219.6(6)	0.2(1)	1665.30[a]	(2^+)
2917.9(4)[a]		1252.6(4)	0.8(2)	1665.30[a]	(2^+)
		1246.6(4)	0.7(2)	1671.34	4^+
		1943.5(4)	3.3(7)	974.34	2^+
2967.4(2)[a]		1042.1(1)	74(4)	1925.23	$(7)^-$
2971.5(3)[a]		363.25(12)	1.4(9)	2608.2[a]	
		560.9(2)	2.5(5)	2410.6	
		1196.7(2)	9.5(7)	1774.69	6^+
		1300.2(2)	4.4(5)	1671.34	4^+
3015.1(3)[a]		406.75(10)	1.6(6)	2608.2[a]	
		907.0(4)	1.4(4)	2108.05	(3,4)
		1227.7(9)	<0.2	1787.6[a]	(2^+)
		1240.1(6)	3(1)	1774.69	6^+
		1343.6(3)	2.0(5)	1671.34	4^+
		2040.8(6)	0.9(3)	974.34	2^+
3091.7(2)		124.2(2)	1.2(4)	2967.4[a]	
		1166.46(13)	22(1)	1925.23	$(7)^-$
3210.4(4)[a]		325.6(3)	2.0(6)	2884.8	
3211.1(3)	(4,5)	356.78(9)	2.8(5)	2854.5[a]	
		723.5(4)	2.3(5)	2487.9	(3,4)
		1103.2(4)	0.5(2)	2108.05	(3,4)
		1436.45(14)	13.4(16)	1774.69	6^+
		1539.6(3)	4.8(14)	1671.34	4^+
3234.8(3)[a]		143.0(3)	0.7(3)	3091.7	
		569.6(5)	3.4(5)	2665.2[a]	
		812.54(10)	4.8(6)	2422.3	
		1181.0(2)	9(1)	2053.88	$(5)^-$
		1309.46(13)	12(1)	1925.23	$(7)^-$
3241.1(5)[a]		273.7(4)	2.3(7)	2967.4[a]	
3254.8(4)[a]		737.3(2)	1.2(8)	2517.4[a]	
3261.0(3)[a]		293.62(7)	18(1)	2967.4[a]	
3305.9(3)		214.22(9)	6(1)	3091.7	
		338.55(9)	9(1)	2967.4[a]	
		1380.7(2)	10(1)	1925.23	$(7)^-$

TABLE II. (*Continued.*)

E_i (keV)	J_i^π	E_γ (keV)	I	E_f (keV)	J_f^π
3335.5(3)[a]		243.7(2)	2.3(8)	3091.7	
		670.3(3)	0.9(4)	2665.2[a]	
		1281.8(3)	2.2(14)	2053.88	$(5)^-$
		1410.2(2)	8(1)	1925.23	$(7)^-$
3350.5(3)[a]		383.2(2)	9(1)	2967.4[a]	
		1425.3(2)	5.6(7)	1925.23	$(7)^-$
3429.4(3)[a]		1321.3(2)	1.1(3)	2108.05	(3,4)
3478.1(3)[a]		172.2(2)	2.6(6)	3305.9[a]	
		510.96(8)	10.9(14)	2967.4[a]	
		1055.96(11)	4.8(9)	2422.3	
		1553.1(2)	7(1)	1925.23	$(7)^-$
3488.3(4)[a]		1380.8(3)	1.6(4)	2108.05	(3,4)
		2513.9(6)	1.7(9)	974.34	2^+
3519.1(3)[a]		552.0(2)	3.0(5)	2967.4[a]	
		1108.5(2)	2.5(6)	2410.6	
3525.1(4)[a]		1114.5(3)	1.3(9)	2410.6	
3562.5(3)	(4^+)	591.09(9)	3.3(7)	2971.5[a]	
		798.2(5)	0.3(2)	2764.37	
		1151.85(16)	21(1)	2410.6	
		1454.5(3)	0.9(4)	2108.05	(3,4)
3593.1(3)[a]		257.61(8)	3.5(5)	3335.5[a]	
		287.1(3)	1.4(10)	3305.9[a]	
		501.3(2)	2.4(6)	3091.7	
		927.9(4)	3.2(6)	2665.2[a]	
		1170.9(2)	13.8(30)	2422.3	
		1667.9(2)	17.9(19)	1925.23	$(7)^-$
3629.4(3)[a]		657.6(3)	1.1(4)	2971.5[a]	
		1076.2(2)	1.7(10)	2553.2[a]	
		1219.0(5)	<0.5	2410.6	
		1521.2(4)	1.4(4)	2108.05	(3,4)
		1854.3(3)	2.5(5)	1774.69	6^+
3660.3(3)[a]		1238.01(2)	4.3(5)	2422.3	
3693.7(4)[a]		1271.4(3)	2.1(9)	2422.3	
		1766.9(3)	14(1)	1925.23	$(7)^-$
3710.3(4)[a]		449.3(1)	4.2(3)	3261.0[a]	
3722.3(5)[a]		1120.7(4)	0.5(2)	2601.8[a]	
		1358.6(4)	0.6(4)	2363.7[a]	(2^+)
3821.1(4)[a]		1056.7(3)	1.4(4)	2764.37	(4,5)
3858.1(2)[a]		2071(1)	<0.2	1787.6[a]	(2^+)
		2187(1)	0.6(3)	1671.34	4^+
3887.1(2)[a]		1523.5(3)	1.2(8)	2363.7[a]	(2^+)
		2100(1)	<0.2	1787.6[a]	(2^+)
		2222(1)	0.5(2)	1665.30[a]	(2^+)
		2912.0(5)	3.5(5)	974.34	2^+
3891.6(3)[a]		1126.5(3)	0.9(4)	2764.37	(4,5)
		1338.8(3)	<1	2553.2[a]	
		1480.1(4)	0.6(2)	2410.6	
		2116.1(4)	1.5(4)	1774.69	6^+
3942.1(3)[a]		730.9(3)	2.4(6)	3211.1	(4,5)
		1087.76(13)	2.7(6)	2854.5[a]	
		1531.6(3)	1.3(3)	2410.6	
		1890(1)	0.6(3)	2053.88	$(5)^-$

TABLE II. (*Continued.*)

E_i (keV)	J_i^π	E_γ (keV)	I	E_f (keV)	J_f^π
3994.8(4)[a]		688.8(2)	3.1(5)	3305.9[a]	
		733.0(3)	1.0(3)	3261.0[a]	
		1027.4(2)	4.3(7)	2967.4[a]	
4001.6(4)[a]		695.9(2)	3.1(5)	3305.9[a]	
		740.5(1)	6.0(6)	3261.0[a]	
		760.4(2)	2.0(8)	3241.1[a]	
		1034.2(2)	3.9(6)	2967.4[a]	
4002.1(3)[a]		1579.8(2)	3.0(10)	2422.3	
4054.9(4)[a]		2280.2(5)	2.1(5)	1774.69	6^+
		2383.6(3)	3.3(14)	1671.34	4^+
4055.4(3)[a]		844.1(2)	1.6(4)	3211.1	(4,5)
		1200.9(13)	0.6(4)	2854.5[a]	
		1291.0(8)	0.2(1)	2764.37	(4,5)
		1502.3(2)	1.5(5)	2553.2[a]	
		1644.5(2)	9(1)	2410.6	
		1947.2(3)	1.8(5)	2108.05	(3,4)
4076.8(3)[a]		2022.9(6)	1.2(11)	2053.88	$(5)^-$
4127.0(3)[a]		1574.0(2)	4.3(5)	2553.2[a]	
		2018.8(5)	2.4(6)	2108.05	(3,4)
		2455(1)	<0.5	1671.34	4^+
4173.8(5)[a]		1409.8(5)	0.5(3)	2764.37	(4,5)
		1763.2(4)	2.2(6)	2410.6	
4260.9(5)[a]		667.9(3)	0.7(3)	3593.1[a]	
		782.5(4)	0.4(2)	3478.1[a]	
		910.2(2)	1.2(4)	3350.5[a]	
		955(1)	0.5(3)	3305.9[a]	
		1169.2(3)	8(1)	3091.7	
		1293.3(3)	1.5(5)	2967.4[a]	
4262.5(5)[a]		568.8(2)	1.6(4)	3693.7[a]	
4305.3(3)[a]		1815.7(4)	0.8(3)	2487.9	(3,4)
		1894.6(4)	0.9(3)	2410.6	
		2197.2(5)	1.3(10)	2108.05	(3,4)
		3329(2)	<0.5	974.34	2^+
4325.2(3)[a]		3351(1)	0.8(5)	974.34	2^+
4337.7(4)[a]		2563.0(3)	3.8(10)	1774.69	6^+
4375.1(4)[a]		1887.2(4)	2.9(9)	2487.9	(3,4)
		2011.3(8)	<0.4	2363.7[a]	(2^+)
		2126(2)	0.7(4)	2248.9[a]	(2^+)
		2587.1(4)	3.6(9)	1787.6[a]	(2^+)
		2703.4(7)	1.2(4)	1671.34	4^+
4382.2(4)[a]		2710.9(7)	2.3(7)	1671.34	4^+
		2717.0(9)	<0.5	1665.30[a]	(2^+)
		3407(2)	0.5(2)	974.34	2^+
4415.3(4)[a]		2166(2)	0.6(4)	2248.9[a]	(2^+)
		2307.4(7)	1.1(4)	2108.05	(3,4)
4433.5(8)[a]		2762.7(8)	0.4(2)	1671.34	4^+
		3459(1)	1.3(7)	974.34	2^+
4439.6(7)[a]		2665.0(6)	1.9(4)	1774.69	6^+
4442.6(5)[a]		440.98(8)	14(1)	4001.6[a]	
		849.5(1)	12(1)	3593.1[a]	
		964.2(2)	7(1)	3478.1[a]	
		1092.0(3)	1.8(6)	3350.5[a]	

TABLE II. (*Continued.*)

E_i (keV)	J_i^π	E_γ (keV)	I	E_f (keV)	J_f^π
		1136.66(18)	0.9(3)	3305.9[a]	
		1181.6(3)	1.3(4)	3261.0[a]	
		1351.05(15)	3.2(6)	3091.7	
		1475.0(3)	1.5(5)	2967.4[a]	
4443.5(6)[a]		750.6(2)	1.4(4)	3693.7[a]	
		2032.7(5)	1.1(5)	2410.6	
4467.7(1)[a]		2219(2)	<0.4	2248.9[a]	(2^+)
		2413.7(7)	<0.5	2053.88	$(5)^-$
		2801(1)	<0.3	1665.30[a]	(2^+)
4468.8(3)[a]		2360.7(5)	0.5(3)	2108.05	
4488.7(5)[a]		493.95(8)	3.4(5)	3994.8[a]	
		1254.1(2)	3.3(6)	3234.8[a]	
		1822.1(4)	0.6(3)	2665.2[a]	
4490.3(5)[a]		796.6(2)	1.8(4)	3693.7[a]	
4513.8(4)[a]		921.1(2)	2.8(7)	3593.1[a]	
		1207.64(18)	2.6(9)	3305.9[a]	
		1422.0(2)	5(1)	3091.7	
4533.0(6)[a]		1924.8(8)	<0.4	2608.2[a]	
		2284.2(5)	<0.4	2248.9[a]	(2^+)
		3558.0(5)	2.7(6)	974.34	2^+
4534.8(7)[a]		841.1(4)	0.9(3)	3693.7[a]	
4584(2)[a]		2797(1)	<0.3	1787.6[a]	(2^+)
		2919.0(8)	1.6(5)	1665.30[a]	(2^+)
		3610(2)	0.7(4)	974.34	2^+
4585.2(5)[a]		2221.5(9)	<0.5	2363.7[a]	(2^+)
		2477.0(3)	2.3(9)	2108.05	(3,4)
4588.5(8)[a]		1238.0(6)	0.2(1)	3350.5[a]	
		1353.95(16)	7(1)	3234.8[a]	
		2166.0(8)	1.3(5)	2422.3	
4604.6(12)[a]		2181.5(9)	<0.4	2422.3	
		2194.0(8)	1.2(5)	2410.6	
		2829.2(7)	1.7(5)	1774.69	6^+
4607.3(8)[a]		1014.25(11)	10(1)	3593.1[a]	
		1129.0(2)	6(1)	3478.1[a]	
		1301.4(3)	1.0(3)	3305.9[a]	
		1346.3(2)	2.4(5)	3261.0[a]	
4654.1(6)[a]		1988.9(4)	1.6(6)	2665.2[a]	
4674(2)[a]		3700(2)	0.3(2)	974.34	2^+
4685.9(5)[a]		2633.0(4)	2.6(5)	2053.88	$(5)^-$
4714.2(4)[a]		1453.2(3)	0.4(2)	3261.0[a]	
4748.9(9)[a]		2695.0(8)	0.6(2)	2053.88	$(5)^-$
4890(2)[a]		2225(1)	0.4(2)	2665.2[a]	

[a]Level was not previously reported.

The new coincidence data show that all three γ rays have alternate placements within the level scheme. Figure 5 shows the present placement of the three transitions, 611, 1309, and 2280 keV; coincident spectra supporting these new placements are given in Figs. 6, 7, and 8, respectively. The intensities measured in the present work are very similar to the previous intensities, making it very unlikely that weak transitions of the same energies still exist in the old placements. Consequently, we removed the 3^- level at 2281 keV from the level scheme of ^{132}Te.

(2_5^+) *at 2364 keV.* A new level at 2364 keV is identified on the basis of two depopulating transitions and four populating transitions. The level is observed to decay to the 2_1^+ state and 0_1^+ state via a 1389.5(2) keV line with intensity 1.2(7) and a 2363.5(3) keV line with intensity 3.6(4), respectively.

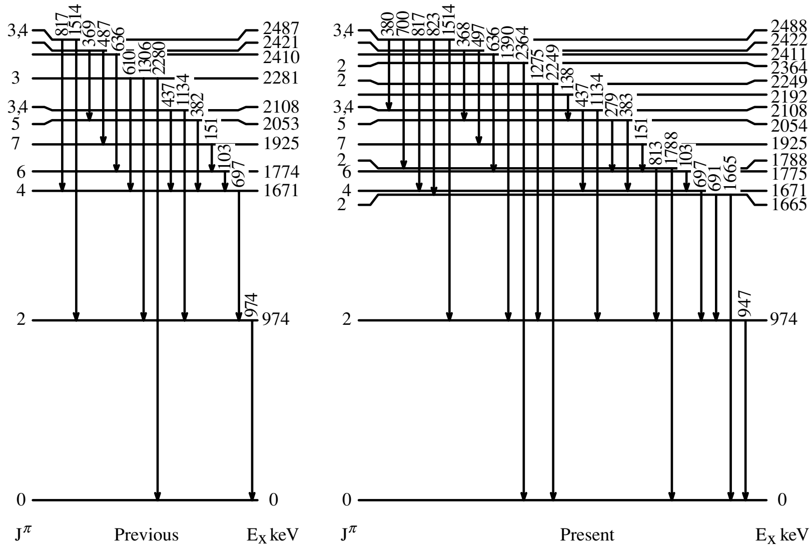

FIG. 2. Low-lying levels in ^{132}Te populated in the present work in ^{132}Sb β^- decay and their depopulating γ-ray transitions with energies in keV (uncertainties ±0.2 keV). For comparison, the left-hand side presents the previous [8] decay scheme.

III. DISCUSSION

^{132}Te, with two protons and two neutron holes relative to the doubly magic ^{132}Sn nucleus, is an excellent case for comparison with shell-model calculations. Detailed shell-model calculations on ^{132}Te were reported in Refs. [4,12]. Taking the model space for both protons and neutrons to be the 50-82 shell, Refs. [4] and [12] give relatively collective structures for the 2_1^+ and 2_2^+ states, while Ref. [12] also gives configurations for the yrast 4_1^+ and 6_1^+ levels, which are primarily proton $|g_{7/2}^2, J\rangle$ excitations. This interpretation is directly supported by the energy levels. A short-range residual interaction acting on a simple two-particle (e.g., $|g_{7/2}^2, J\rangle$) structure for all these yrast states would give a closely lying triplet of levels $2_1^+, 4_1^+, 6_1^+$ with $R_{4/2} \sim 1.2$. The fact that the

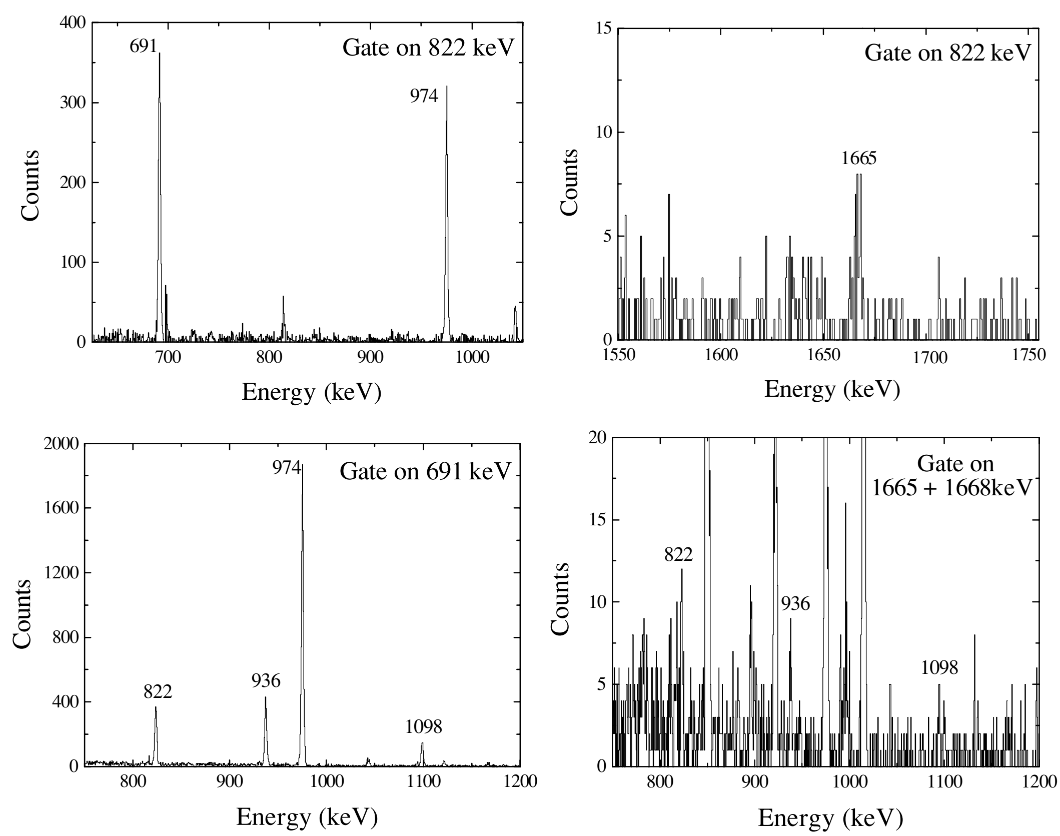

FIG. 3. Gated coincidence spectra providing evidence for a new level at 1665 keV. Note that the 1665 keV transition lies on the shoulder of a much stronger 1668 keV transition; therefore, coincidences with the 1668 keV line are also observed in the figure.

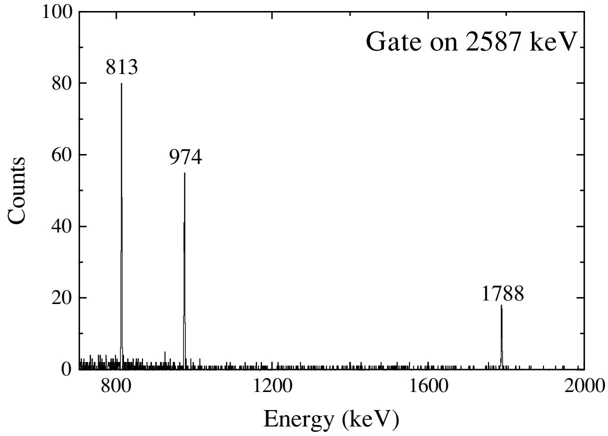

FIG. 4. Gated coincidence spectra providing evidence for a new level at 1788 keV. Spectra gated on the 2587 keV transition allegedly feeding the level at 1788 keV showing coincidences with 813 and 1788 keV depopulating transitions.

2^+_1 energy is well below the 4^+_1 state ($R_{4/2} \sim 1.7$) supports the collective aspect of the 2^+_1 level.

The new levels at 1665, 1788, 2249, and 2364 keV are tentatively assigned as 2^+. Since each of these levels is observed to decay only to the 0^+_1 and 2^+_1 states, spin assignments are restricted to $1^{\pm}$ or 2^+, assuming $E1$, $M1$, or $E2$ deexcitation transitions. However, below about 3 MeV, $1^{\pm}$ levels are unlikely. Both the protons and neutrons are filling the single-particle orbitals of the 50-82 shell. Since positive parity orbits have $J_{\max} = 7/2$ and the negative parity states must involve the $1h_{11/2}$ orbit, a two-particle 1^- configuration cannot be formed. Thus any 1^- level must have seniority $\nu \geqslant 4$ and

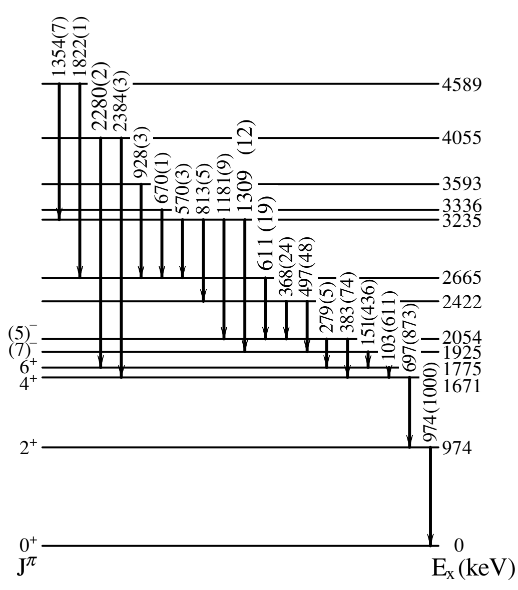

FIG. 5. Partial decay scheme of ^{132}Te showing the present placement of the three transitions (highlighted) at 611, 1309, and 2280 keV, which previously were reported to depopulate a 3^- level at 2281 keV. Included are only the levels and transitions relevant to the new placements. Each transition is labeled by its energy in keV and relative intensity.

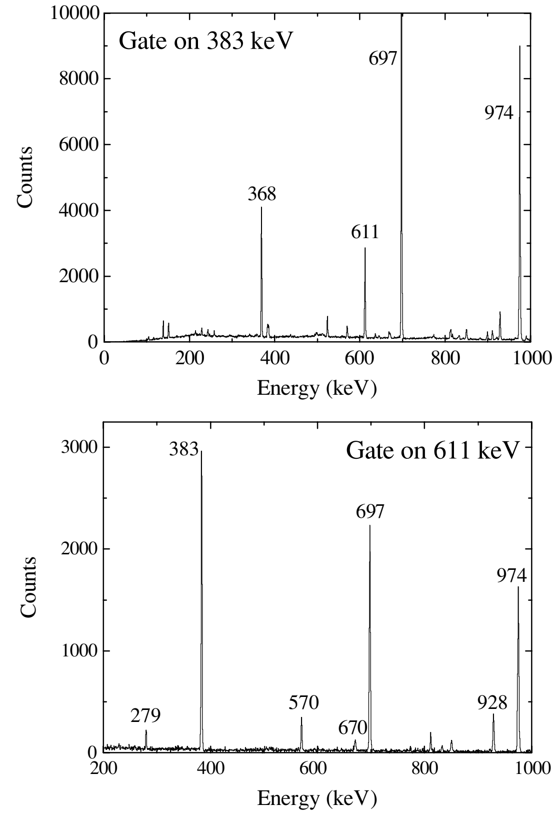

FIG. 6. Spectra gated on the 383 and 611 keV transitions supporting the new placement of the 611 keV transition.

should be quite high lying. For the protons filling the bottom of the shell, a two-quasiparticle 1^+ state can be formed with the configuration $|\pi\ 2d_{5/2}\ 1g_{7/2}\rangle$. Assuming a short-range residual interaction, this configuration would give a sequence of levels $6^+, 4^+, 2^+$ $(1^+, 3^+, 5^+)$ with the 6^+ lowest in energy and the odd-spin states degenerate at higher energies. For neutrons filling the top of the shell, the available configuration for a two-quasiparticle 1^+ state is $|\nu\ 1d_{3/2}\ 2s_{1/2}\rangle$. Here spins of only 1^+ and 2^+ are permitted, and again assuming a short-range residual interaction, the 1^+ would lie above the 2^+ in energy. Since all possible configurations place the $1^{\pm}$ states high in

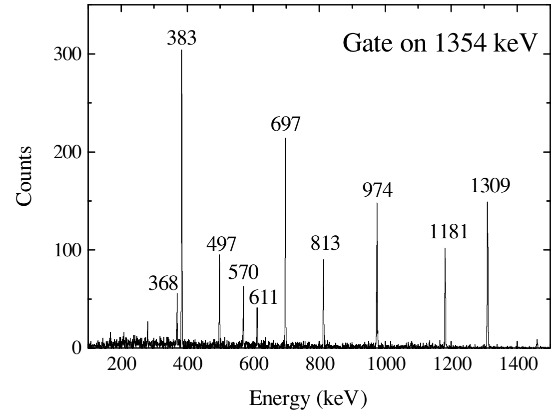

FIG. 7. Spectrum gated on the 1354 keV transition supporting the new placement of the 1309 keV transition.

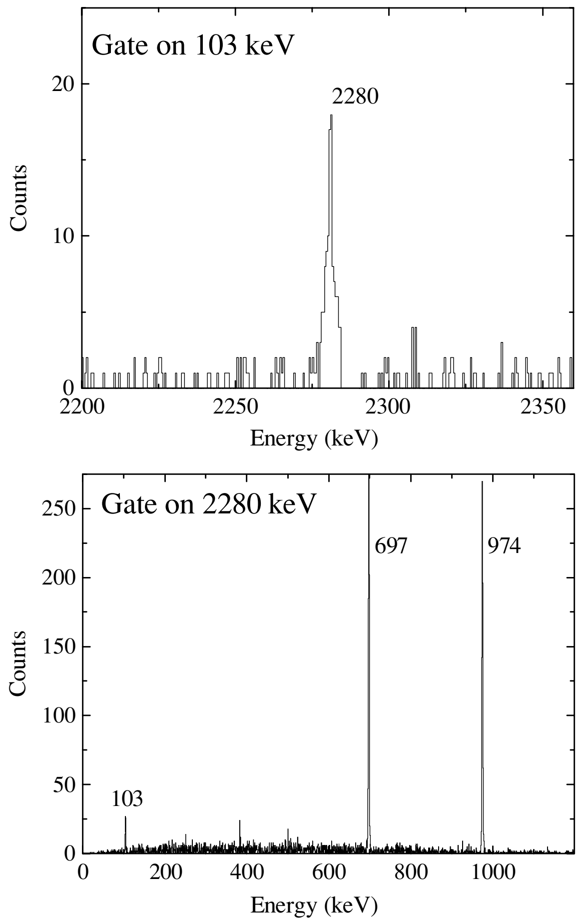

FIG. 8. Spectra gated on the 103 and 2280 keV transitions supporting the new placement of the 2280 keV transition.

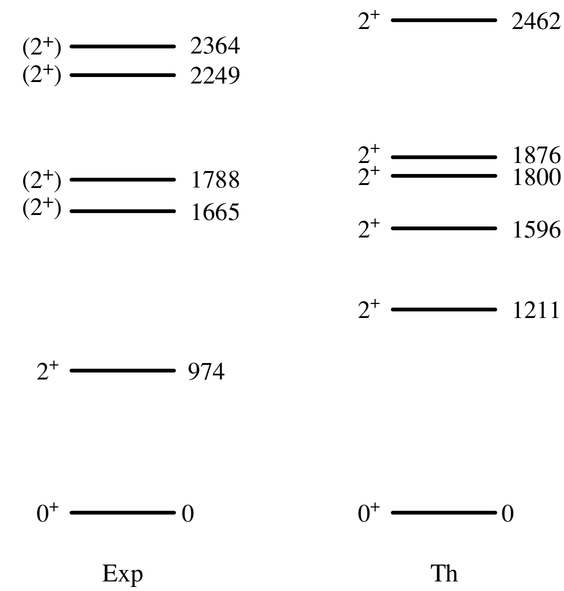

FIG. 9. Comparison of experimental and theoretical [13] 2^+ state energies in ^{132}Te.

energy, we tentatively assign $J^- = 2^+$ to these new levels, although one of the higher states could be the $|\nu\ 1d_{3/2}\ 2s_{1/2};\ J = 1^+\rangle$ state mentioned above.

In an effort to reproduce the properties of the 2_1^+ state below and above $N = 82$ in Sn and Te nuclei, Terasaki *et al.* [4] used different densities of neutron single-particle levels below and above $N = 82$. The $E(2^+)$ and $B(E2; 0^+ \rightarrow 2^+)$ values are not symmetric adjacent to $N = 82$: both the 2_1^+ energy and $B(E2; 0^+ \rightarrow 2^+)$ value in ^{132}Te are higher than in ^{136}Te, contradicting simple systematics and general intuition about quadrupole collectivity. This anomalous behavior was explained [4] using an enhanced neutron pairing before the $N = 82$ magic gap in comparison with that above it. A comparison of all the 2^+ energies with those predicted [13] with the procedure outlined in Ref. [4] was made in Ref. [5] and is shown in Fig. 9. The agreement is quite good, with the theory predicting the correct number of low-lying 2^+ levels at approximately the observed energies.

The lowest negative parity states can also have a simple shell-model interpretation. The 5_1^- and 7_1^- states were described [8,12] as originating from two-neutron configurations. As an argument in favor of the neutron assignment for the 7_1^- state, Ref. [8] cited the extremely hindered $E1$ decay $7^- \rightarrow 6^+$ $[\nu 1h_{11/2}2d_{3/2} \rightarrow \pi(g_{7/2}^2)] \sim 10^{-9}$ W.u. [9].

The neutron excitation nature of the 7_1^- and 5_1^- levels is supported by an overall analysis of the possible negative parity simple configurations. Negative parity excitations for both protons and neutrons must involve the $1h_{11/2}$ orbit. The positive parity partner of this orbit is for neutrons, either the $2d_{3/2}$ or the $3s_{1/2}$ orbits; and, for protons, the $2d_{5/2}$ and $1g_{7/2}$ orbits. Table III gives the multiplet sequences for these four configurations with a short-range attractive interaction [14]. The sequence 7^- to 5^- could correspond to the $|1h_{11/2}1g_{7/2}J\rangle$ proton configuration or the $|1h_{11/2}2d_{3/2}J\rangle$ neutron configuration. The first one would have a 9^- below the 7^- and 5^-. However, there is no evidence for a low-lying 9^- level, so the only possible simple configuration for the 7_1^- and 5_1^- levels is, indeed, the neutron excitation. This argument is consistent with the qualitative results of Ref. [12]. This type of configuration implies also the existence of nearly degenerate 6^- and 4^- levels. The level at 2422 keV was assigned 6^- [10] and is likely part of this multiplet. Again, this is consistent with Ref. [12].

Concerning the 3^- level, only the proton excitations $|1h_{11/2}2d_{5/2}J\rangle$ include this spin. Our new coincidence data

TABLE III. Negative parity multiplets and expected level ordering.

Configuration	J values	Multiplet levels in expected order of increasing energy[a]
Protons		
$1h_{11/2}2d_{5/2}$	3–8	3, 5, 7, (4, 6, 8)
$1h_{11/2}1g_{7/2}$	2–9	9, 7, 5, 3, (2, 4, 6, 8)
Neutrons		
$1h_{11/2}3s_{1/2}$	5, 6	5, 6
$1h_{11/2}2d_{3/2}$	4–7	7, 5, (4, 6)

[a]Assuming a short-range, attractive residual interaction. Levels expected to be nearly degenerate are grouped in parentheses.

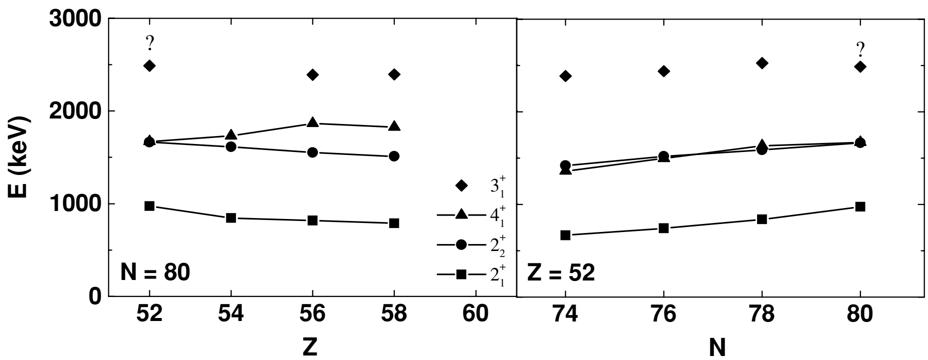

FIG. 10. Energies of selected low-lying states in Te isotopes.

found no evidence for the previously reported 3^- state at 2281 keV. Based on observed depopulating transitions, the lowest energy candidate for a 3^- state is the level at 2488 keV, although spins of 3^+ and $4^\pm$ are also possible. This energy fits quite well with the octupole excitations in the region [15] as shown in Fig. 10 for both the isotopic and isotonic chains of ^{132}Te, where the 2488 keV level is labeled with a question mark. Included in Fig. 10 is the evolution of the 2_1^+, 2_2^+, 4_1^+, and 3_1^- level energies. In the case of the 2_2^+ level, the smooth trends include the candidate at 1665 keV in ^{132}Te, which constitutes further support for this assignment.

IV. CONCLUSION

Levels in ^{132}Te were populated in β^- decay of a ^{132}Sb radioactive beam. Information obtained through high-efficiency γ-ray coincidence spectroscopy led to a major revision of the decay scheme of ^{132}Te relative to the previously published work. The new 2^+ low-lying levels are interpreted in terms of the recent quasiparticle random-phase approximation (QRPA) calculations. A new 3_1^- level is also proposed.

ACKNOWLEDGMENTS

The work is supported by U.S. DOE Grant nos. DE-FG02-91ER-40609, DE-FG02-88ER-40417, and DE-FG02-91ER-40608. Research at the Oak Ridge National Laboratory is supported by the U.S. Department of Energy under Contract No. DE-AC05-00OR22725 with UT-Battelle, LLC. We are especially grateful to Witek Nazarewicz and to J. Terasaki for discussions of the calculations in Ref. [4] and to J. Terasaki for providing detailed predictions [13] from those calculations that are not included in Ref. [4]. We thank B. Walters for informing us of Ref. [10] and P. Regan and E. Henry for useful discussions.

[1] D. C. Radford *et al*., Eur. Phys. J. A **15**, 171 (2002).
[2] D. C. Radford *et al*., Phys. Rev. Lett. **88**, 222501 (2002).
[3] C. J. Barton *et al*., Phys. Lett. **B551**, 269 (2003).
[4] J. Terasaki, J. Engel, W. Nazarewicz, and M. Stoitsov, Phys. Rev. C **66**, 054313 (2002).
[5] R. O. Hughes *et al*., Phys. Rev. C **69**, 051303(R) (2004).
[6] C. J. Gross *et al*., Nucl. Instrum. Methods Phys. Res. A **450**, 12 (2000).
[7] M. A. Caprio *et al*., Phys. Rev. C **66**, 054310 (2002).
[8] A. Kerek, P. Carle, and S. Borg, Nucl. Phys. **A224**, 367 (1974).
[9] Yu. V. Sergeenkov, Nucl. Data Sheets **65**, 277 (1992).
[10] R. A. Meyer and E. A. Henry (unpublished; private communication).
[11] J. Bryssinck *et al*., Phys. Rev. C **59**, 1930 (1999).
[12] J. Sau, K. Heyde, and R. Chery, Phys. Rev. C **21**, 405 (1980).
[13] J. Terasaki *et al*. (private communication).
[14] R. F. Casten, *Nuclear Structure from a Simple Perspective* (Oxford University Press, New York, 2000).
[15] R. H. Spear, At. Data Nucl. Data Tables **42**, 55 (1989).